Caving 2026 – A van As, D Cumming-Potvin & J Wesseloo (eds)
© 2026 Australian Centre for Geomechanics, Perth, ISBN 978-1-7636842-3-2
doi:10.36487/ACG_repo/2645_80

Influence of testing configuration on the behaviour of energy-absorbing, self-drilling rockbolts under impact loading

Greig Knox [a,*], **John Hadjigeorgiou** [b]

[a] *Epiroc, South Africa*

[b] *University of Toronto, Canada*

Abstract

A major challenge in block caving operations is the selection of ground support that can accommodate the deformation associated with the significant stress changes during the life of an operation. This is best accomplished using high energy-absorbing rockbolts. An additional operational constraint is the installation of the selected rockbolts in heavily fractured or poor ground conditions. Under these constraints, the use of energy-absorbing, self-drilling rockbolts becomes an attractive option.

The ISRM suggested method for determining the performance of energy-absorbing rockbolts in the laboratory relies on dropping a given mass from a specific height employing 2 testing configurations to transfer the kinetic energy of the falling mass to the rockbolt that is installed in a steel tube. The continuous tube configuration simulates an impact load directly applied onto the rockbolt plate while the split tube represents a loading condition on a rockbolt when a rock block is ejected by an impact thrust. The in situ loading of a rockbolt under seismic loads is more complex. This paper investigates the influence of the split location along the testing tube on the behaviour of energy-absorbing, self-drilling rockbolts. The results of this experimental program demonstrated that the location of the split within the host tube controlled both the maximum plate displacement and dissipated energy recorded prior to the rupture of the rockbolt. These additional loading configurations contribute to an improved understanding of the behaviour of Energy-absorbing Self-drilling Rockbolts under impact loading. This has significant practical implications for the selection and design of ground support in block caving operations.

Keywords: *hollow core rockbolts, impact testing, split location*

1 Introduction

A major challenge in block caving operations is the selection of ground support that can accommodate the deformation associated with the significant stress changes during the life of an operation. This is best accomplished using high energy-absorbing reinforcement and yielding surface support. Energy-absorbing rock reinforcement elements are designed to be resilient to large deformations. Their capacity of sustaining a load over large displacements is a major advantage over conventional reinforcement elements. The mechanical behaviour of energy-absorbing rockbolts under load has been established through several laboratory-based quasi-static and impact loading test campaigns. A limitation of these tests has been that in most cases the loading configuration has been axial, through either direct or indirect loading split tube method (Simser 2007; Li 2010; Li & Doucet 2012; Player 2012; Knox & Berghorst 2018; Li et al. 2021; Vallati et al. 2022). These testing campaigns have provided meaningful insight into the performance capacity of energy-absorbing rockbolts under axial loading in a controlled laboratory environment. However, field observations suggest that the location, direction and rate of loading can vary significantly. This can explain variations in performance of energy-absorbing rockbolts. The influence of the split location was demonstrated for a paddled energy-absorbing rockbolt by Knox & Hadjigeorgiou (2022), with a 90% variance

* Corresponding author email: greig.knox@epiroc.com

in the capacity of the rockbolt. This paper aims to address the knowledge gap associated with different impact loading configurations for energy-absorbing, self-drilling rockbolts.

2 Energy-absorbing self-drilling rockbolts

Energy-absorbing or yielding rockbolts are routinely used to support large loads and deformations associated with mining-induced seismicity and squeezing ground conditions. Currently, there are multiple energy-absorbing rockbolts commercially available (Hadjigeorgiou 2024). The effectiveness of these rockbolts, however, can be limited due to installation issues in poor ground conditions resulting in poor quality boreholes and resin migration in heavily fractured ground (Knox & Hadjigeorgiou 2023). The use of self-drilling rockbolts can potentially overcome these installation limitations.

The renewed interest in self-drilling rockbolts as part of primary support in mining applications coincides with the development of specialised bolting equipment (Faulkner et al. 2017; Bray et al. 2019) that meet the desired mining rates (Jere et al. 2023). This facilitated the installation rates that are compatible with primary support installation rates, rejuvenating a need for an energy-absorbing rockbolt that can be successfully installed in poor ground conditions. Equivalent rockbolts that overcome the installation challenges and provide adequate energy-absorbing capacity have recently been developed by several ground support suppliers (Jennmar 2022; Minova 2026; Normet 2026; Epiroc 2022).

A typical energy-absorbing, self-drilling rockbolt consists of hollow bar with a drill bit affixed to the distal end of the rockbolt, as illustrated in Figure 1. The length of the threaded section of the rockbolt is matched to the strength characteristics of the chemical anchor employed to couple the rockbolt to the borehole. The yielding mechanism employs a highly deformable section of smooth bar, bounded by anchors mechanically coupled with a resin or cementitious grout, that elongates when load is applied.

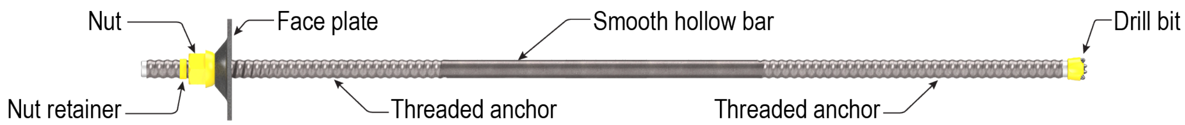

Figure 1 Illustration of an energy-absorbing, self-drilling rockbolt

2.1 Installation of an energy-absorbing, self-drilling rockbolt using pumpable resin

Hollow core rockbolts – of which energy-absorbing, self-drilling rockbolts are a subset – can be installed with either a one-step installation or a two-step installation. In highly fractured rock masses, a one-step installation (Figure 2) – where the rockbolt replaces the drill string – results in higher operational efficiency.

The energy-absorbing, self-drilling rockbolt is coupled to the rockdrill allowing the transfer of percussive energy to the carbide buttons of the drill bit fixed at the distal end of the rockbolt. The drilling process employs a combination of percussion and rotation applied to the proximal end of the rockbolt. In a hard rock environment, water is continually flushed through the hollow core of the rockbolt to clear the fractured rock from the distal end of the borehole. The rockbolt is drilled to the correct depth when the washer plate makes firm contact with the rock mass. At this stage, the rockdrill is decoupled from the rockbolt. Following this step, resin is injected through the core of the rockbolt, to the distal end of the borehole, filling the annulus between the rockbolt and the borehole. At this point resin is visible at the periphery of the face plate. Post-injection of resin ensures that variations in hole size and the presence of voids surrounding the rockbolt are accommodated, to achieve a full column bond, as illustrated in Figure 3. The installation of the energy-absorbing, self-drilling rockbolt is completed following a short resin curing period during which the rockbolt is held in place by the bolter.

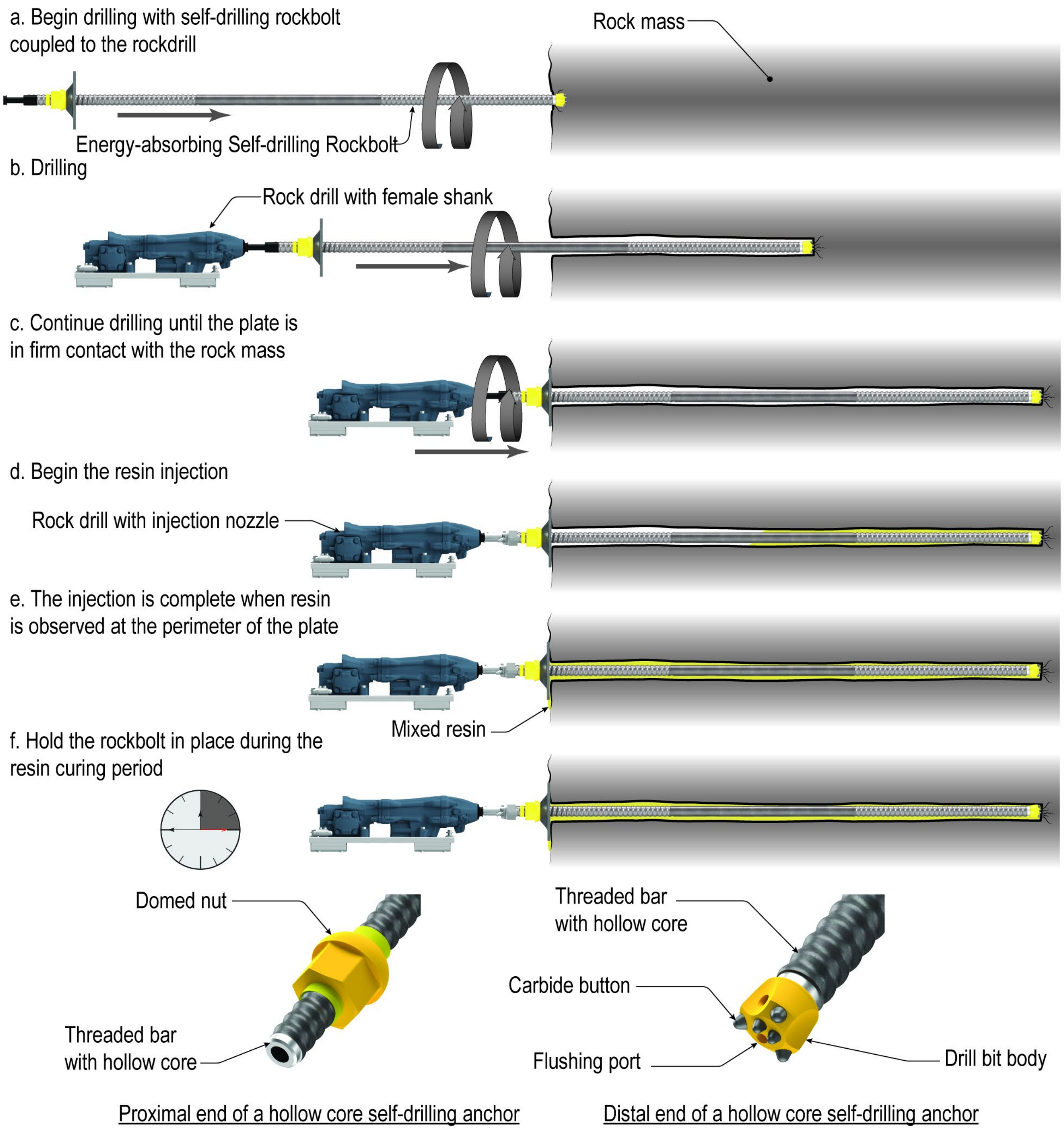

Figure 2 Installation procedure for an energy-absorbing, self-drilling rockbolt (after Knox & Hadjigeorgiou 2023)

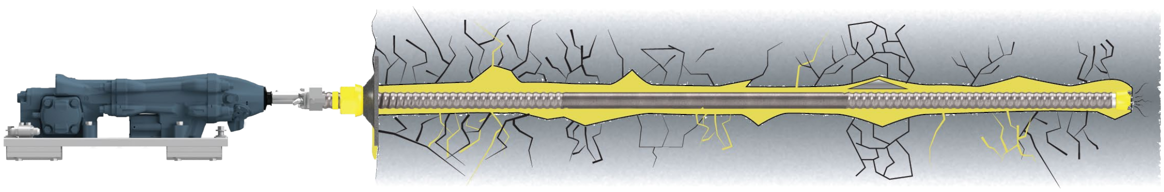

Figure 3 Post-grouting compensation for variations in borehole profile (Knox & Hadjigeorgiou 2023)

The combination of self-drilling installation and post-grouting with a rapid curing chemical medium ensures the consistency of installation over a range of rock mass conditions. A constraint is the requirement for specialised bolting equipment, resin systems and associated costs, limits the current application to special projects, such as rehabilitation in extreme ground conditions where the application of ground support using conventional methods is impossible.

3 Mechanical behaviour of hollow core self-drilling rockbolts

Knox & Hadjigeorgiou (2023) have previously investigated the mechanical behaviour of hollow core self-drilling rockbolts under quasi-static conditions. The focus in this paper is its behaviour under impact loads. Laboratory-based impact testing provides a method of determining the response of the rock reinforcement element to high strain rate events (>10^0 s^{-1}) and is often a prerequisite for the adoption of a new energy-absorbing rock reinforcement element at mine sites. However, prior to the work of Punkkinen & Royer (2022) and Abreu & Knox (2022), there is an absence of available impact test performance data for yielding self-drilling energy-absorbing rockbolts. Abreu & Knox (2022) investigated the influence of the drilling cycle on the performance of an R28 energy-absorbing, self-drilling rockbolt, which was demonstrated through a series of 47 kJ indirect impact central split tube impact tests. This revealed a 33% reduction in its energy dissipation capacity when compared with samples that had not been drilled to depth. Consequently, the reduction in capacity was attributed to the effect of the percussive force applied to the drill steel during drilling.

A compilation of the published impact performance data compiled from multiple sources (Abreu & Knox 2022; Evans 2022; Punkkinen & Royer 2022; Holden et al. 2024; Jennmar 2024) is presented in Figure 4. This illustrates the performance in trends but it should be recognised that differences in rockbolt geometry and testing configuration can influence the results. This was highlighted in a benchmarking study by Li et al. (2021) where a degree of testing rig bias was identified between rigs.

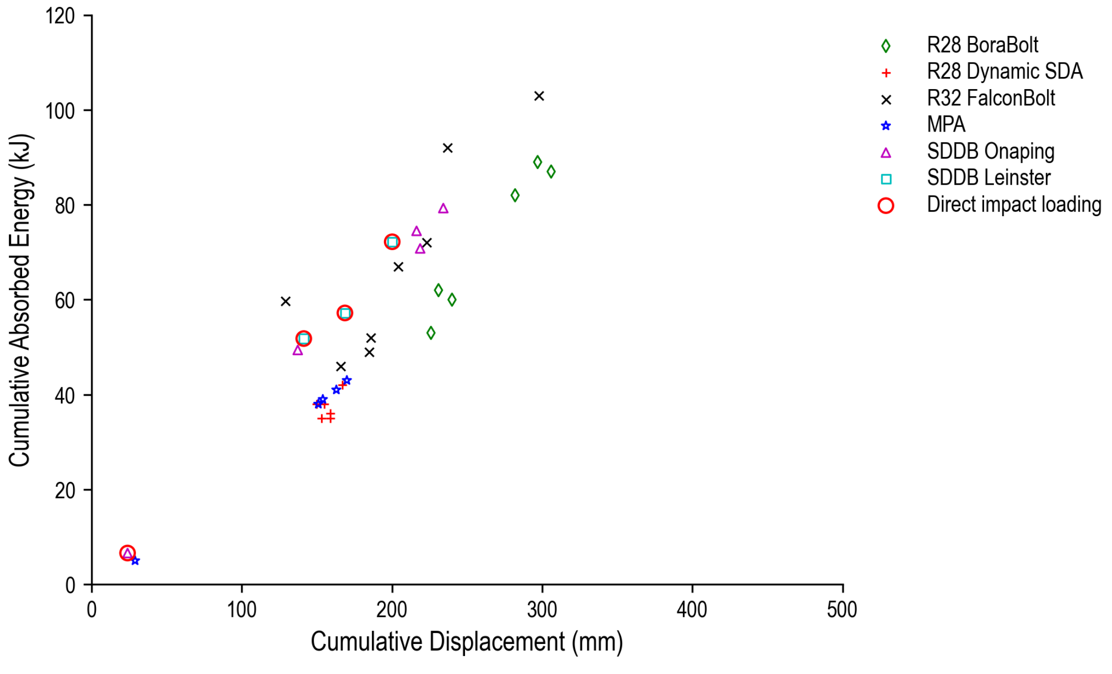

Figure 4 Summary of cumulative displacement versus absorbed energy impact test data for common energy-absorbing, self-drilling rockbolts

Punkkinen & Royer (2022) investigated the response of an R32 energy-absorbing, self-drilling rockbolt under both indirect central split tube and direct impact continuous tube loading. The rockbolts were subjected to a series of 19 kJ impact tests. Two variants of the rockbolt defined by the length of the thread anchor portion were tested, with rupture typically occurring in the deformable length of hollow steel. The failure of the bond in the proximal threaded anchor, coupled with the non-standard installation of the accessories limits the applicability of the test results in defining the performance capacity of the rockbolt. Of concern is the triple nut installation during testing as shown in Figure 5 (Punkkinen & Royer 2022). The collapse of the plate as reflected in the load-displacement response, suggest that the capacity of the interface between the proximal anchor and the chemical anchor was exceeded. In effect the loading response could be considered to be equivalent to that of a point anchored rockbolt and similar to a direct impact response.

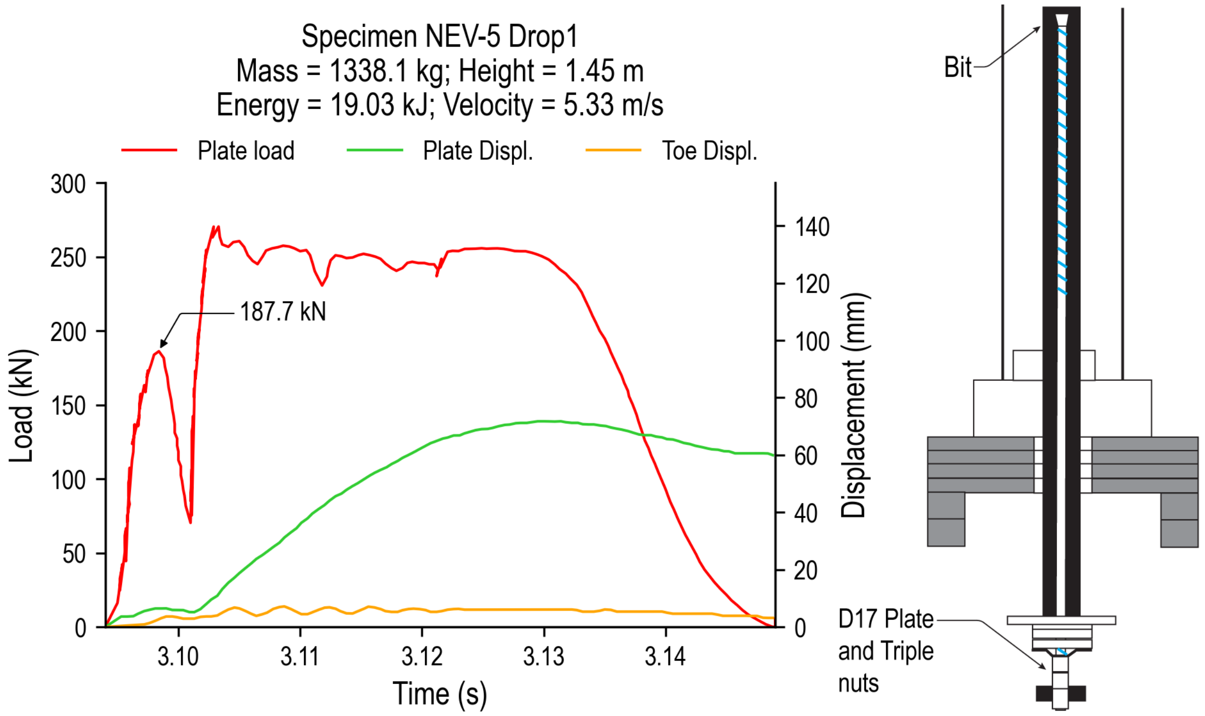

Figure 5 Impact load-displacement response for a 'Nevada' style SDDB bolt (Punkkinen & Royer 2022)

A field installation of an energy-absorbing, self-drilling rockbolt typically employs tightening of the bolt and face place using a single nut as shown in Figure 6. The application of 3 nuts, depicted in Figure 5, used during the impact load of the energy-absorbing, self-drilling rockbolt is not representative of field applications and questions the validity of extrapolating the laboratory results to typical field conditions.

Figure 6 An example of an installed energy-absorbing, self-drilling rockbolt illustrating the application of the rockbolt with a single nut (Watt et al. 2018)

Holden et al. (2024) investigated the dynamic performance of an R32 energy-absorbing self-drilling rockbolt when subjected to a series of 30 and 50 kJ indirect impact central split tube tests. A total of 8 samples of 2 different configurations were tested, all with cumulative plate displacement ranging from 166 to 298 mm.

Since the introduction of specialised installation equipment (Bray et al. 2019), interest in the application of self-drilling rockbolts has increased. Nevertheless, there is an absence of quantifiable and applicable performance data under complex loading. This is addressed in the present work.

4 Experimental program

Laboratory-based impact load testing provides a controlled environment for assessing the capacity of a rockbolt when subjected to high strain rates associated with seismic events. These events typically result in a demand which exceeds the capacity of conventional ground support elements resulting in rupture of tendons or failure of the elements connecting the tendons or a system failure with failure of both the surface support and the rockbolts. Given that energy-absorbing, self-drilling rockbolts have only recently been trialled at mine sites, there are very limited empirical performance data on their behaviour under seismic loading. This underscores the importance of laboratory investigations to get an insight into rockbolt performance under impact loads.

The impact testing program was specifically designed to quantify the influence of testing configuration, split location, on the performance of the specified energy-absorbing rockbolts. Split location was found to be critical in investigating the performance of paddled energy-absorbing rockbolts.

Prior work on energy-absorbing, self-drilling was limited to the two conventional configurations: the direct impact continuous tube (see Figure 7a) and the indirect impact split tube impact configuration (see Figure 7c) where the split was located centrally along the length of the deformable section bounded by the 2 anchor points. This comprehensive investigation employed 3 additional configurations to quantify the effect of the split location and the impact configuration on the performance of the rockbolt, with the rationale adopted from Knox & Hadjigeorgiou (2022). All impact tests configurations are illustrated in Figure 7.

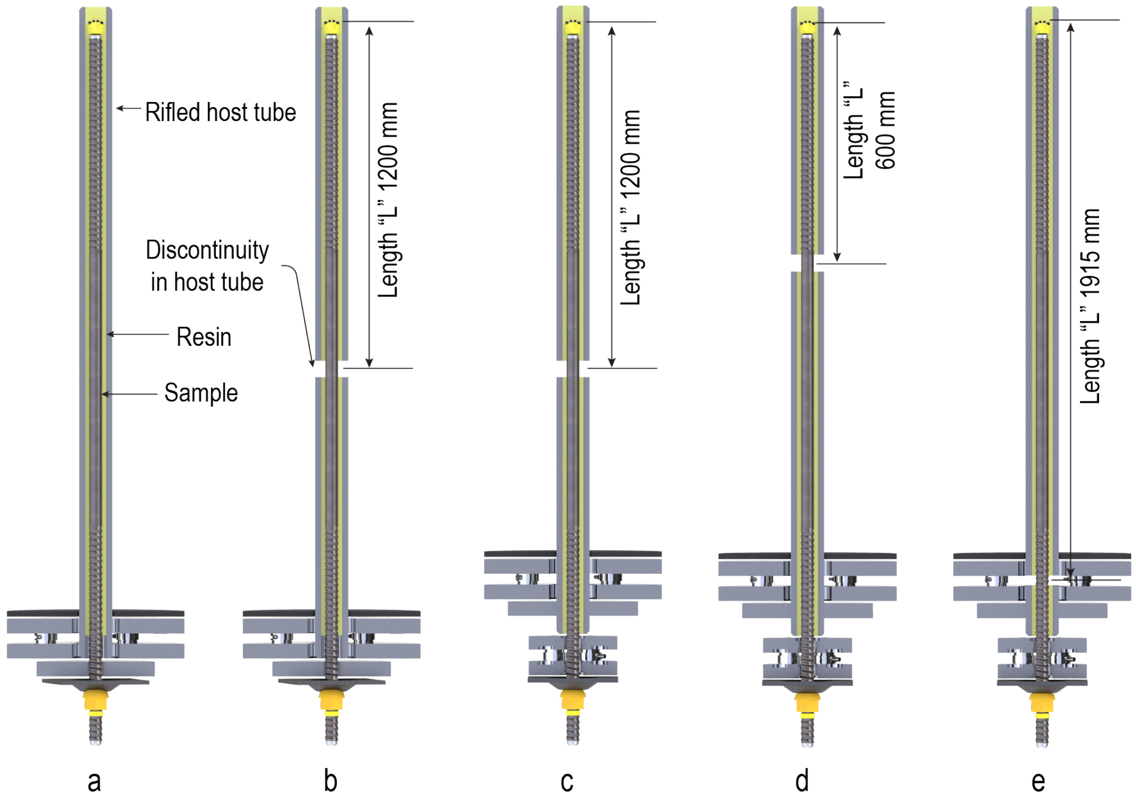

Figure 7 Split location along the tube for both direct and indirect impact test configurations. (a) Direct impact continuous tube; (b) Direct impact split tube; (c) Indirect impact split tube; (d) Indirect impact critical embedment length split tube; (e) Indirect impact anchor split tube

The rockbolt is configured and instrumented for a direct impact loading configuration as illustrated in Figure 7 and in Figure 8b, where a discontinuity (split) is introduced into the host tube centrally located between the two anchor points (1,200 mm from the distal end of the rockbolt). Consequently, the nut-thread interface and the deformable section are both loaded, and the rupture will occur in the weakest of the 2 elements. The second and third configurations were instrumented for an indirect impact test. The split in the host tube was introduced at the proximal end of the distal anchor, as shown in Figure 7d, and constituted a critical embedment impact test. In the last configuration, a split was introduced in the proximal anchor at approximately 1,915 mm from the distal end of the rockbolt, as shown in Figure 7e.

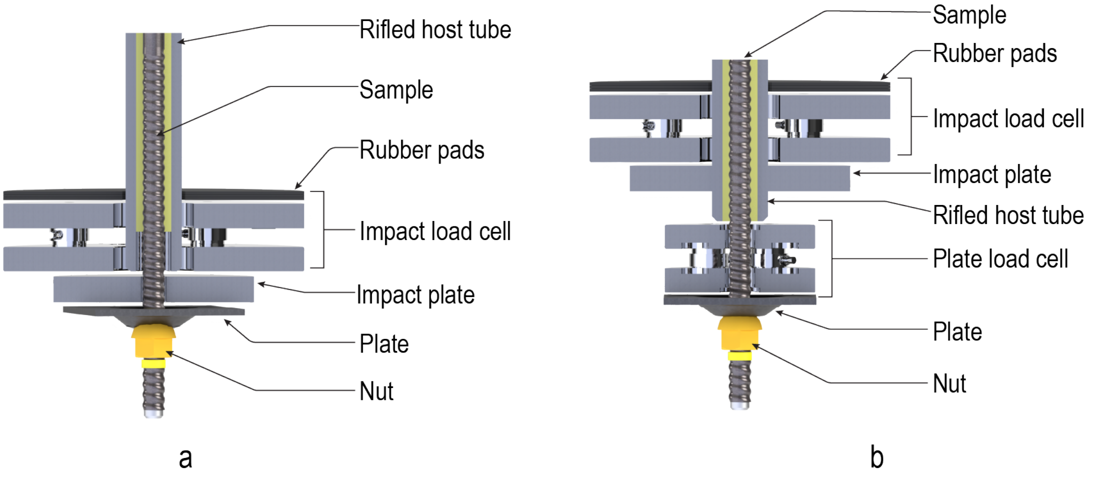

Figure 8 Loading configuration instrumentation for impact testing of paddled energy-absorbing rockbolts. (a) Direct impact loading; (b) Indirect impact loading

The host tubes, Ø36 mm internal diameter with a 10 mm wall thickness, were rifled with a trapezoidal profile with 2 mm depth, 4 mm width, on a 12 mm pitch.

4.1 Specifications of the energy-absorbing, self-drilling rockbolt

For this investigation an R28 BoraBolt energy-absorbing, self-drilling rockbolt was selected, as illustrated in Figure 9. This was the same rockbolt previously used in quasi-static investigations by Knox & Hadjigeorgiou (2023). The R28 BoraBolt is an energy-absorbing, self-drilling rockbolt produced from a Ø28 mm hollow bar with a Ø15 mm internal diameter. As illustrated in Figure 9, the BoraBolt employs the typical design of an energy-absorbing, self-drilling rockbolt, with a deformable section bounded by two threaded anchors.

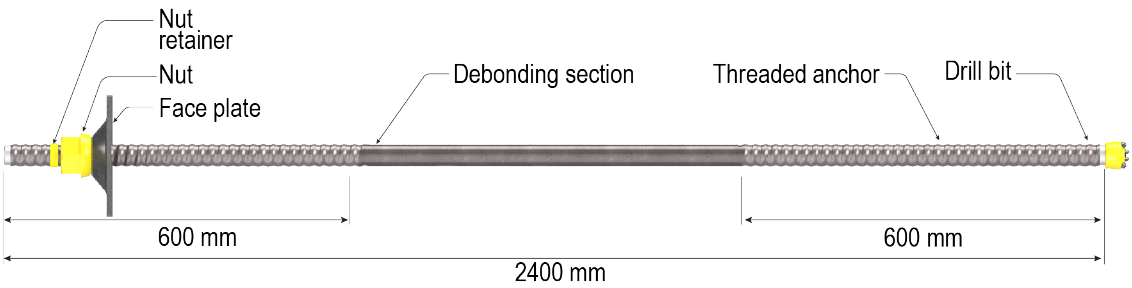

Figure 9 Illustration of the R28 BoraBolt energy-absorbing, self-drilling rockbolt configuration (Knox & Hadjigeorgiou 2023)

The energy dissipation mechanism comprises plastic deformation of the smooth (highly deformable) section between the threaded anchor sections which decouples from the grouting medium (resin) and elongates when load is applied to the rockbolt. The thread anchor length for this variant of the energy-absorbing, self-drilling rockbolt is 600 mm. The length of the anchor may vary dependent on the supplier or the properties of the chemical anchor.

5 Experimental results and analysis

Fifteen full-scale impact tests (2.4 m rockbolts) were conducted in batches of 3 samples as defined in Table 1. For example, SD-CT refers to a self-drilling direct impact continuous tube impact configuration. The input energy was maintained at 30 kJ throughout the experimental program (≈2,000 kg from a height of 1.5 m). All rockbolts were subjected to multiple impact loads resulting in either rupture of the sample or failure of the load transfer mechanism.

Table 1 Impact loading configuration description and sample references nomenclature

	Configuration	Host tube configuration	Reference
Conventional configurations	Direct impact	Continuous: no split (Figure 7a)	SD-CT
	Indirect impact	Central split: 1,200 mm from distal end of host tube (Figure 7c)	SD-12ST
Extended configurations	Direct impact	Central split: 1,200 mm from distal end of host tube (Figure 7b)	SD-DST
	Indirect impact	Distal split: 600 mm from distal end of host tube (Figure 7d)	SD-06ST
	Indirect impact	Proximal split: centrally located in the embedded length of the proximal anchor. 1,915 mm from the distal end of the host tube (Figure 7e)	SD-AST

The results for each batch are summarised below, including post-rupture image of the samples. Selected response curves are shown in Figure 10 and are separated into conventional configurations which were described in detail by Li et al. (2021) and extended impact test configurations presented by Knox & Hadjigeorgiou (2022). The complete summary of the individual results is presented in Table 2. A distinct reduction in the capacity of the rockbolt is observed when the split is located towards the proximal end of the rockbolt (SD-CT, SD-DST, SD-AST). This was governed by the capacity of the proximal thread.

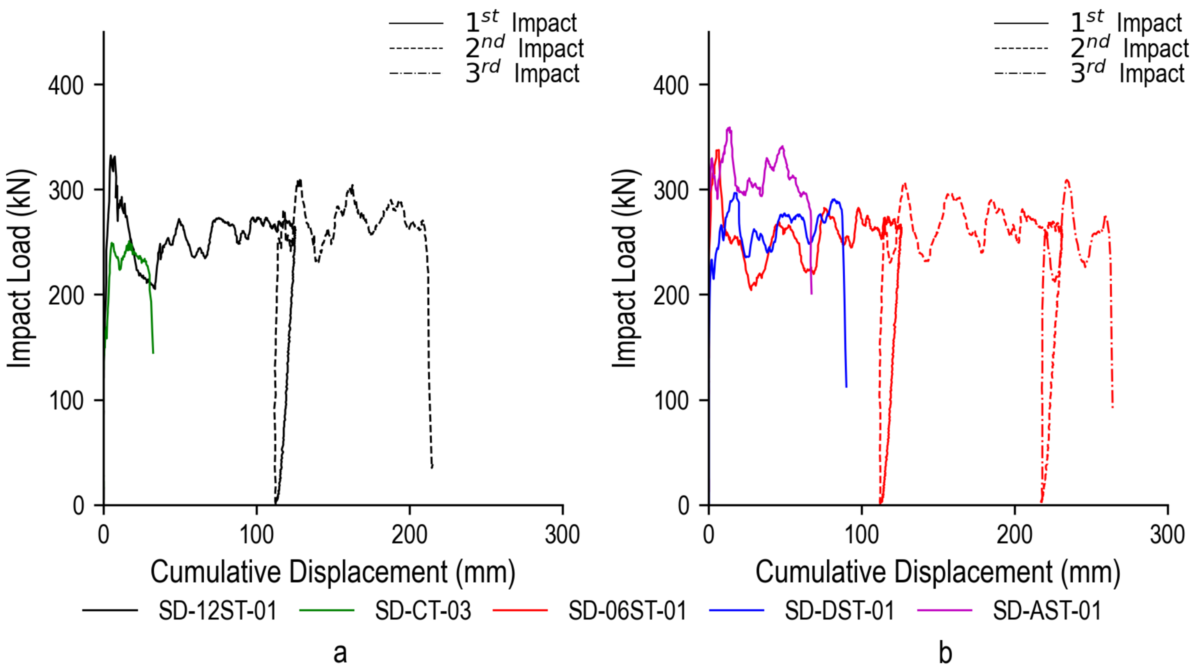

Figure 10 Typical impact load–displacement responses for the 5 loading configurations. (a) Conventional impact test configurations; (b) Extended impact test configurations

Table 2 Summary of the impact test results for all configurations

Sample reference	Number of impacts	1st impact			2nd impact			3rd impact			δ_{p_t}	PE_t^I
		δ_{p_f}	$\bar{F}_{IMP}$	PE_1^I	δ_{p_f}	$\bar{F}_{IMP}$	PE_2^I	δ_{p_f}	$\bar{F}_{IMP}$	PE_3^I		
SD-CT-01	1	41	254	10							41	10
SD-CT-02	1	34	221	7							34	7
SD-CT-03	1	33	233	7							33	7
SD-12ST-01	2	113	260	31	103	267	27				215	58
SD-12ST-02	2	113	249	30	86	257	22				199	52
SD-12ST-03	2	115	252	30	84	268	22				199	52
SD-DST-01	1	90	264	23							90	23
SD-DST-02	1	94	256	24							94	24
SD-DST-03	1	83	246	20							83	20
SD-06ST-01	3	112	258	31	105	266	30	46	251	11	264	72
SD-06ST-02	3	115	254	31	107	267	31	51	272	14	274	75
SD-06ST-03	3	116	297	37	109	313	37	58	303	17	282	91
SD-AST-01	1	67	312	21							67	21
SD-AST-02	2	119	284	35	86	315	26				205	61
SD-AST-03	2	118	298	36	41	78	16				159	52

δ_{p_f} (mm); $\bar{F}_{IMP}$ (kN); PE_n^I (kJ)

The direct impact continuous tube configuration was originally used to quantify the performance under strainbursting conditions (Li et al. 2021). The load is applied directly to the accessories of the rockbolt and subsequently the plate, plate-nut and the thread-nut interface are all loaded during the impact test. The inadequate capacity of the thread–nut interface directly limited performance of the rockbolt under direct loading conditions, with 2 out of the 6 direct impact tests (3 by direct impact continuous tube and 3 by direct impact central split tube) resulting in stripping of the thread-nut interface, as shown in Figures 11 and 12.

The observed failure mode of stripping of the nut-thread interface results from the geometric profile of the thread, larger pitch (12.7 mm) with a shallow profile (1.7 mm depth) and a relatively wide tolerance band in the thread-nut interface. A minor reduction in the thread diameter, which is frequent in ductile materials, results in a reduction in the shear area of the thread. The consequence was a stripping failure in the thread-nut interface.

Figure 12 illustrates 2 cases of thread stripping and one of ruptured thread. As with Knox & Hadjigeorgiou (2022) under quasi-static loads, the load capacity of the threaded portion of the rockbolt governed the capacity of the rockbolt. The threaded portion of the rockbolt ruptured with a decrease in deformation of the central deformable section when compared to the indirect impact central split tube (SD-12ST) and the indirect impact distal split tube (SD-06ST) configurations.

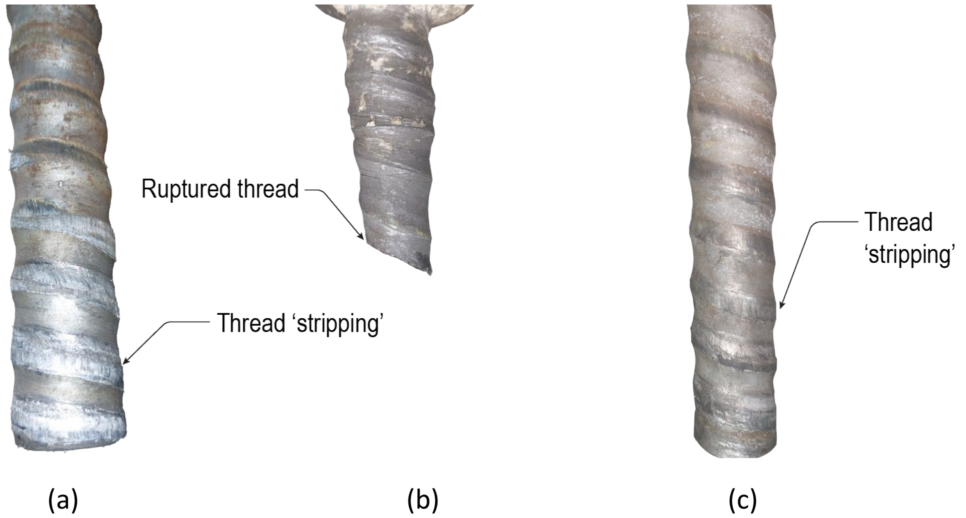

Figure 11 Rupture/failure interface for the 3 direct impact continuous tube impact tests. (a) Thread stripping (SD-CT-01); (b) Ductile necking and rupture of the thread (SD-CT-02); (c) Stripping of the thread–nut interface (SD-CT-03)

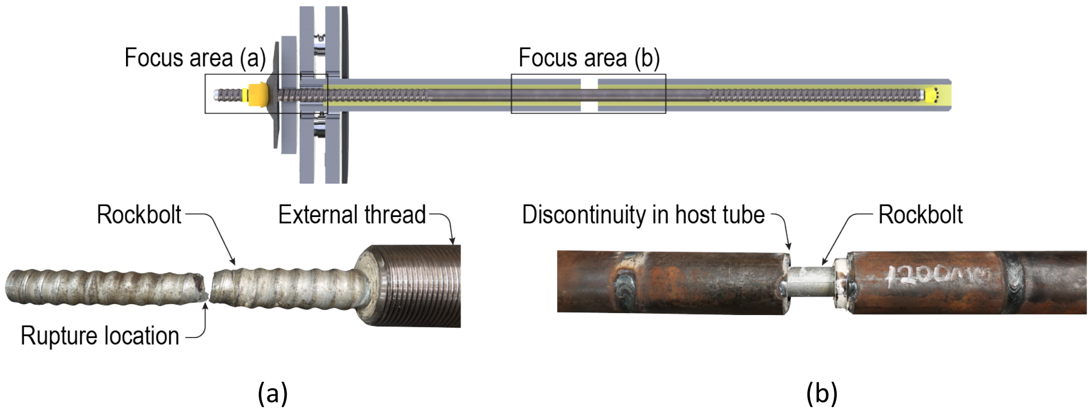

Figure 12 Rupture location for the direct impact split tube configuration. (a) Rupture location in the thread of the rockbolt; (b) Deformation that occurred between the anchor points

The indirect impact tests resulted in deformation of the central section of the rockbolt in 8 of the 9 tests, in Figures 13–15. A ductile cup and cone rupture interface was observed in the samples which is consistent with the behaviour of a purely axially loaded tendon. Under indirect impact central split tube loading, the rockbolt sustained the first impact, rupturing on the second. An increase in capacity was observed in the indirect impact distal split tube loading when compared with the indirect impact split tube loading. The rockbolts consistently sustained 2 impacts before rupturing on the third. This is an inverse of the relationship reported by Knox & Hadjigeorgiou (2022) for paddled energy-absorbing rockbolts, highlighting the importance of laboratory investigations for each rockbolt type. While the energy dissipation mechanisms of the paddled energy-absorbing rockbolt and the energy-absorbing, self-drilling rockbolts are the same, the difference in anchoring medium and rockbolt configuration resulted in an inversion of the response.

As observed, with the indirect impact anchor split tube (SD-AST) configuration, the resin-anchor interface was overloaded, which resulted in a loading of the central deformable stem (SD-AST-02,-03). The threaded portion of the rockbolt was loaded in sample SD-AST-01 which resulted in the reduction in recorded deformation and energy capacity.

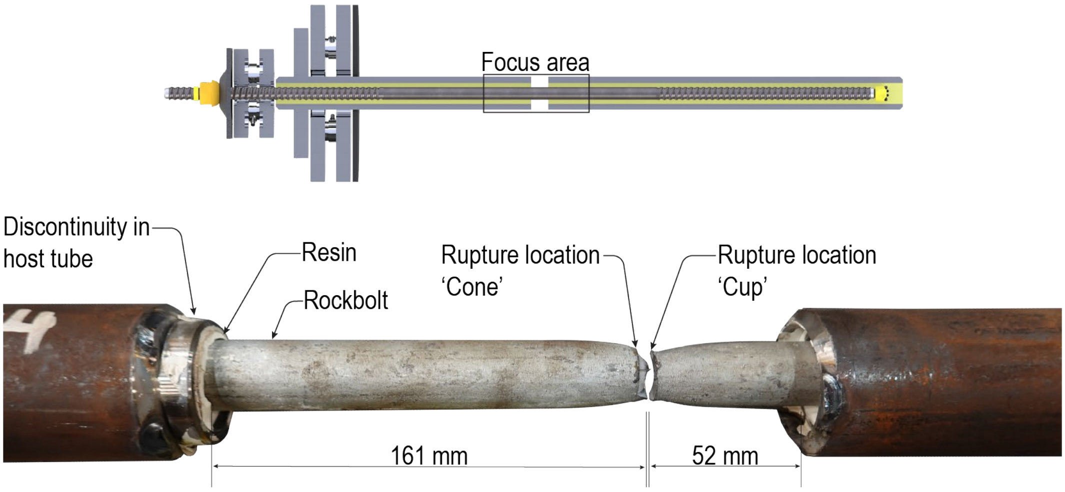

Figure 13 Typical ductile necking and rupture location observed resulting from an impact test using an indirect impact split tube loading for the energy-absorbing, self-drilling rockbolt

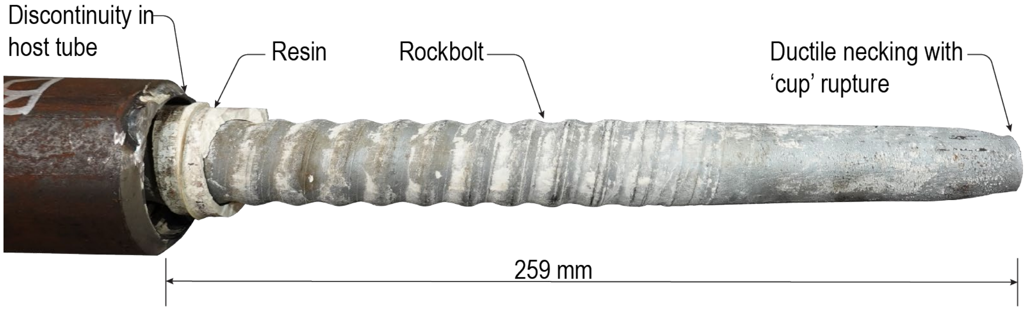

Figure 14 Rupture of the bar post-distal split tube impact loading

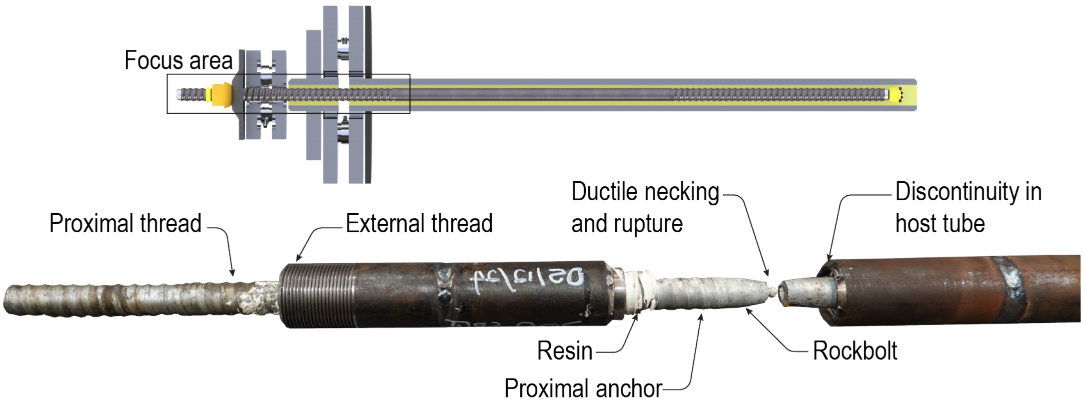

Figure 15 Bar rupture post the proximal anchor split tube impact loading

6 Discussion

The energy-absorbing, self-drilling rockbolt and the paddled energy-absorbing rockbolt share the same design principle. They both employ a deformable smooth bar chemically anchored by 2 or more geometric features with a threaded element at the proximal end for the attachment of accessories. It was therefore anticipated that the influence of the impact loading configuration and the split location would be similar.

A total of 15 rockbolts were used in this investigation into the influence of the impact loading configuration and split location on the capacity of the energy-absorbing, self-drilling rockbolt. The response of the rockbolts to the loading configurations is summarised in Figure 10 and Table 3. Due to the rockbolt design (i.e. inferior nuts and thread), a lower capacity was recorded for the direct impact continuous tube configuration (8 kJ) when compared with the indirect impact split tube configuration (54 kJ). This is due to the difference in the length of mobilised bar. The decreased thread load capacity exacerbates the reduction in rockbolt performance. This is also evident in the difference in reduced energy capacity between the direct impact split tube test (22 kJ) and the indirect impact split tube test. The typical rupture interface, for direct impact loading, was the nut–thread interface or in the threaded feature, as illustrated in Figure 11. This is further evidence that the load capacity of the thread governs the capacity of the rockbolt during direct impact loading. The process of producing the thread results in a reduction in load capacity of the threaded section when compared with the anchor and hollow bar portions of the rockbolt. It can be concluded that a direct impact loading method highlights the shortcoming in the design of the rockbolt as evident by a reduction in the recorded capacity of the rockbolt. Conventional wisdom dictates that this would be the loading case in the event of a strainburst event.

The relocation of the split location over the length of the rockbolt resulted in a difference of 34 kJ when comparing the indirect impact test with the split located in the proximal anchor (45 kJ) and the split located at the proximal end of the distal anchor (79 kJ). However, the total difference when the effect of both the impact loading configuration and the split location are combined would be 71 kJ. The lowest recorded energy absorption capacity was 8 kJ for the direct impact continuous tube.

Table 3 Average impact plate displacement and energy absorption capacity of the for R28, 2.4 m energy-absorbing, self-drilling rockbolt per impact configuration

	Configuration	Host tube configuration	Batch reference	$\overline{\delta}_p$ (mm)	$\overline{PE}_t^I$ (kJ)
Conventional configurations	Direct impact	Continuous: no split	SD-CT	36	8
	Indirect impact	Central split: 1,200 mm from distal end of host tube	SD-12ST	204	54
Extended configurations	Direct impact	Central split: 1,200 mm from distal end of host tube	SD-DST	89	22
	Indirect impact	Distal split: 600 mm from distal end of host tube	SD-06ST	273	79
	Indirect impact	Proximal split: centrally located in the embedded length of the proximal anchor. 1915 mm from the distal end of the host tube	SD-AST	144	45

The observed rupture location for the different impact test configurations after the test is graphically represented in Figure 16. The location of the rupture provides insight into the strain distribution during impact loading. Once the location of the rupture had been recorded, a number of the samples were selected to be cross-sectioned.

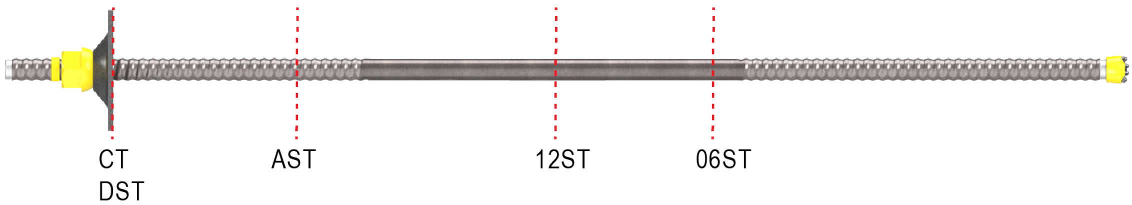

Figure 16 Observed rupture location for the energy-absorbing, self-drilling rockbolt for each of the 5 impact testing configurations

No damage to the resin annulus between the rockbolt and the host tube was visible in dissections of the tested rockbolt samples. However, some fractures of the resin inside the rockbolt were observed in dissections of both the indirect impact centrally located split SD-12ST (Figure 17) and the split located at the proximal end of the distal paddle set SD-06ST (Figure 18). The frequency of observed fracturing was higher for the sample from the 06ST batch, likely resulting from the proximity of the section relative to the split in the tube.

Of interest is the plastic deformation of the anchor portion of the rockbolt, which is visible in the anchor split sample SD-AST Figure 19; however, it is also visible in samples from both the indirect impact central split tube SD-12ST (Figure 17) and the indirect impact with the split located at the proximal end of the distal anchor SD-06ST (Figure 18).

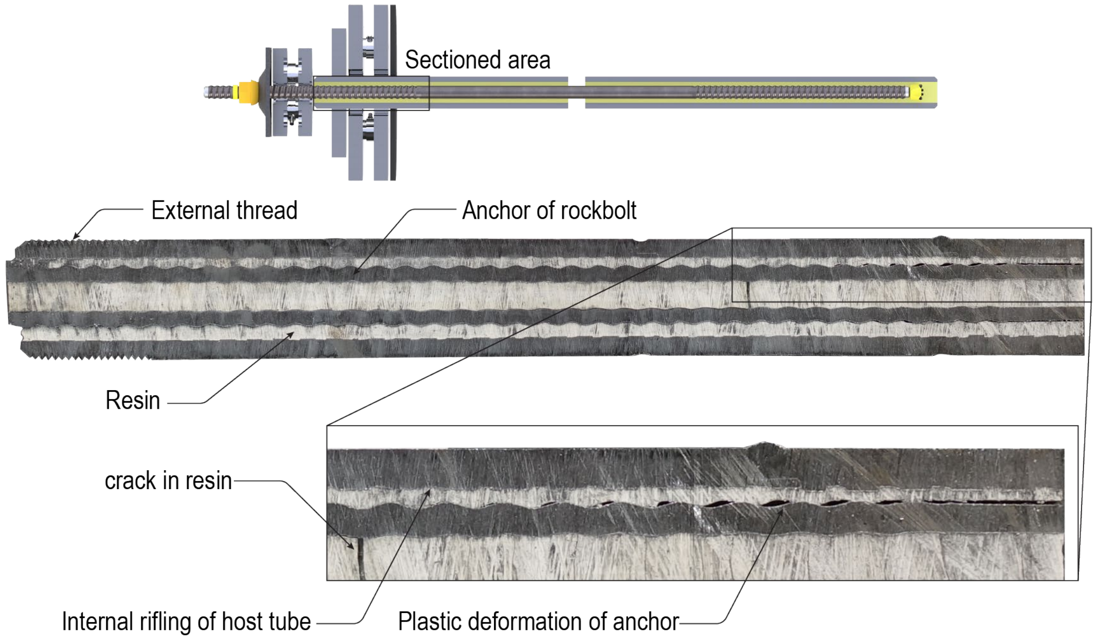

Figure 17 SD-12ST-02: plastic deformation of the proximal anchor

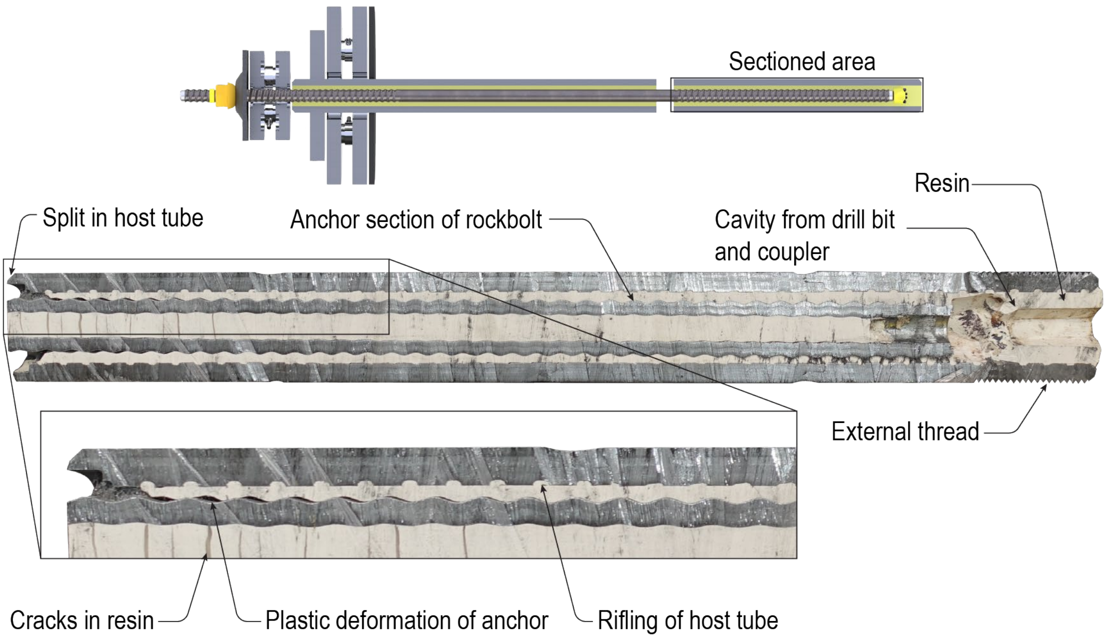

Figure 18 SD-06ST02: plastic deformation of the threaded anchor. No movement of the distal anchor observed

The cavity seen on the right-hand-side of the anchor in Figure 18 is from the drill bit and coupler which is affixed to monitor distal displacement (i.e. the displacement of the samples relative to the host tube). The absence of damage to the resin suggests that the 600 mm bond length was an adequate embedment length.

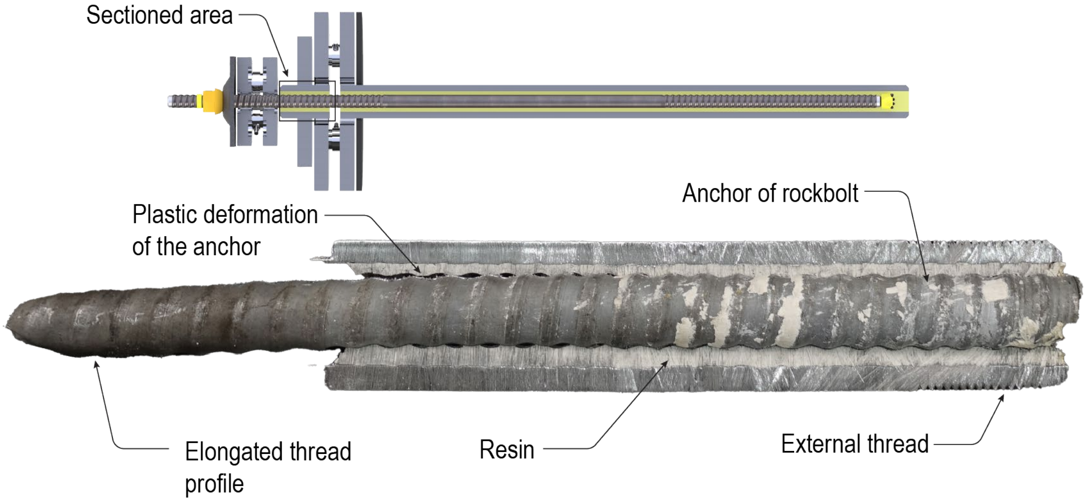

Figure 19 SD-AST-01: plastic deformation of the proximal anchor

7 Conclusion

Heavily fractured and broken rock masses often present a challenge for the effective installation of ground support. The use of self-drilling rockbolts can potentially overcome this. The development of specialised bolting equipment capable of installing self-drilling rockbolts, in combination with a rapid curing 2 component resin, resulted in the use of self-drilling rockbolts as part of the ground support cycle in mines in recent years.

Energy-absorbing, self-drilling rockbolts have also recently been introduced for application in seismic and squeezing ground conditions. Confidence in their use is hindered by the absence of quality data as to their behaviour under complex loading. Although several investigations provide data as to the capacity of energy-absorbing, self-drilling rockbolts under axial loading, there is an absence of data of its performance under more complex loading conditions. An experimental program was therefore developed to quantify the effect of the impact loading configuration on the performance of energy-absorbing, self-drilling rockbolts.

The results of that investigation, as presented in this paper, highlight the importance of conducting a rigorous laboratory testing program. Due to the similarity in the design concepts of the paddled energy-absorbing rockbolt and the energy-absorbing, self-drilling rockbolts the influence of the split location on the performance of the rockbolt was expected to be aligned with the response reported by Knox & Hadjigeorgiou (2022) for paddled energy-absorbing rockbolts. Although similarities were observed in the relationship between the direct impact and the indirect impact configurations, a distinct difference was observed in the influence of the split located within the deformable section of the rockbolt.

References

Abreu, R & Knox, G 2022, 'The influence of drilling on the performance of a yielding self-drilling rockbolt', in Y Potvin (ed.), *Caving 2022: Proceedings of the Fifth International Conference on Block and Sublevel Caving*, Australian Centre for Geomechanics, Perth, pp. 165–176, https://doi.org/10.36487/ACG_repo/2205_09

Bray, P, Johnsson A, & Shcunnesson, H 2019, 'Rock reinforcement solutions case study: Malmberget iron ore mine, Sweden', in W Joughin (ed.), *Proceedings of the Ninth International Conference on Deep and High Stress Mining* The Southern African Institute of Mining and Metallurgy, Johannesburg, pp. 191–204.

Epiroc 2022, *BoraBolt*, viewed 20 May 2022, https://www.epiroc.com/en-za/products/rock-drilling-tools/ground-support/energy-absorbing-rockbolts/borabolt

Evans, DW 2022, 'Data cross validation for a newly commissioned dynamic drop test facility', *Proceedings of The Fifth Australasian Ground Control in Mining Conference Proceedings*, The Australasian Institute of Mining and Metallurgy, Melbourne, pp. 320–328.

Faulkner, D, Stankus, J, Ma, K & Ma, L 2017, 'Multiple point anchor (MPA), self-drilling, hollow core yielding bolt with injectable J-lok P resin system for high-stress and squeezing ground conditions', *Proceedings of the 51st U.S. Rock Mechanics/Geomechanics Symposium*, American Rock Mechanics Association, Alexandria.

Hadjigeorgiou, J 2024, 'Inconvenient truths about ground support in deep and high-stress mines', in P Andrieux & D Cumming-Potvin (eds), *Deep Mining 2024: Proceedings of the 10th International Conference on Deep and High Stress Mining*, Australian Centre for Geomechanics, Perth, pp. 23–60, https://doi.org/10.36487/ACG_repo/2465_0.02

Holden, M, Akdag, S, Chengguo, Z, Oh, J, Saydam, S, Galluzzi, R & MacDonald, D 2024, 'Dynamic performance testing and numerical modelling of the falcon bolt', in *New Challenges in Rock Mechanics and Rock Engineering*, CRC Press, Boca Raton, pp. 859–865.

Jennmar 2022, *MPA Bolt System*, viewed 20 May 2022, https://www.jennmar.com/products/mpa-bolt-system

Jennmar 2024, *MPA Bolt System Brochure,* https://www.jennmar.com/products/mpa-bolt-system

Jere, P, Battison, R & Arnold, M 2023, 'Performance of fully mechanised rock reinforcement using self-drilling anchors', in *Underground Operators Conference 2023: Conference Proceedings*, Australasian Institute of Mining and Metallurgy, Melbourne, pp. 258–268.

Knox, G & Berghorst, A 2018, 'Increased agility for the research and development of dynamic roof support products', in CC Li, XB Li & ZX Zhang (eds), *Proceedings of Rock Dynamics – Experiments, Theories and Applications*, CRC Press, Trondheim, pp. 373–384.

Knox, G & Hadjigeorgiou, J 2022, 'Influence of testing configuration on the performance of paddled energy-absorbing rockbolts under impact loading', *Rock Mechanics and Rock Engineering*, vol. 55, pp. 5705–5721.

Knox, G & Hadjigeorgiou, J 2023, 'Performance of conventional and energy-absorbing self-drilling hollow core rockbolts under controlled laboratory conditions', *Rock Mechanics and Rock Engineering*, vol. 56, pp. 4363–4378.

Li, C 2010, 'A new energy-absorbing bolt for rock support in high stress rock masses', *International Jounrnal of Rock Machanics & Mining Sciences*, vol. 47, pp. 396-404.

Li, CC & Doucet, C 2012, 'Performance of D-bolts under dynamic loading conditions', *Rock Mechanics and Rock Engineering*, vol. 45, pp. 193–204.

Li, C, Hadjigeorgiou, B, Mikula, P, Knox, G, Darlington, B, Royer, R … Hosp, M 2021, 'Performance of identical rockbolts tested on four dynamic testing rigs employing the direct impact method', *Journal of Rock Mechanics and Geotechnical Engineering*, vol. 13, no. 4, pp. 745–754.

Minova 2026, *Uni-pass Bolting System,* viewed 29 June 2026, https://www.minovaglobal.com/product/unipass-dynamic-bolt/

Normet 2026, *Self-Drilling Anchors*, viewed 29 June 2026, https://www.normet.com/en/products-and-services/rock-reinforcement/dynamic-bolts/self-drilling-dynamic-bolt-sddb

Player, JR 2012, *Dynamic Testing of Rock Reinforcement Systems*, PhD thesis, Curtin University of Technology, Perth.

Punkkinen, A & Royer, R 2022, 'Performance of Normet self drilling dynamic bolt (SDDB) types in dynamic loading - the energy dissipating hollow core rockbolt installed in Norment's urea-silicate injection resin', in *RASIM2022*, Society for Mining, Metallurgy & Exploration, Englewood.

Simser, BP 2007, 'The weakest link - ground support observations at some Canadian Shield hard rock mines', in Y Potvin (ed.), *Deep Mining 2007: Proceedings of the Fourth International Seminar on Deep and High Stress Mining*, Australian Centre for Geomechanics, Perth, pp. 335–348, https://doi.org/10.36487/ACG_repo/711_25

Vallati, O, Darlington, B & Sandberg, L 2022, 'Dynamic drop testing of Sandviks D47 and D39 MDX bolts at the Swerim's testing facility', *Proceedings of The Fifth Australasian Ground Control in Mining Conference Proceedings*, The Australasian Institute of Mining and Metallurgy, Melbourne, pp. 428–440.

Watt, G, Roberts, T & Faulkner, D 2018, 'Single pass drill, install and inject self-drilling resin bolt applications in poor ground', *Proceedings of The Fourth Australasian Ground Control in Mining Conference Proceedings*, The Australasian Institute of Mining and Metallurgy, Melbourne, pp. 323–343.